

# Actionable Three-Phase Infeasibility Optimization with Varying Slack Sources

Elizabeth Foster<sup>1\*</sup>, Timothy McNamara<sup>1</sup>, Amritanshu Pandey<sup>1,2</sup> and Larry Pileggi<sup>1</sup>

<sup>1</sup> Electrical & Computer Engineering, *Carnegie Mellon University*, Pittsburgh, PA

<sup>2</sup> Electrical & Computer Engineering, *University of Vermont*, Burlington, VT  
{emfoster, tmcnama2, amritanp, pileggi}@andrew.cmu.edu

**Abstract**—Modern distribution grids that include numerous distributed energy resources (DERs) and battery electric vehicles (BEVs) will require simulation and optimization methods that can capture behavior under infeasible operating scenarios to assess reliability. A three-phase infeasibility analysis is based on localizing and identifying power deficient areas in distribution feeders via a non-convex optimization that injects and subsequently minimizes slack sources, subject to AC network constraints. In our power flow optimization, we introduce and compare three different representations for slack resources: current, power, and admittance. Operational bounds are incorporated to ensure realistic solutions for all cases. We find that the slack power formulation converges fastest across our testcases of up to 1599 nodes, and both slack power and slack admittance generally return smaller net power requirements for network feasibility as compared with slack current models. Formulations with slack power models and slack admittance models are demonstrated to effectively represent reactive power compensation on a taxonomy feeder.

**Index Terms**—distribution grid optimization, three-phase infeasibility analysis, voltage bounds, optimal power flow

## I. INTRODUCTION

Modern electric grids are seeing an influx of distributed energy resources (DERs) and smart technologies like battery electric vehicles (BEVs) at the distribution level [1] [2] [3]. These new resources and technologies present opportunities to achieve climate goals, amongst other benefits; however, they also present new challenges as system planners attempt to build out the infrastructure required to incorporate these assets while maintaining grid reliability and resiliency [2] [3].

System planners use tools that are generally limited to traditional methods like three-phase power flow, which outputs nodal voltages and line/transformer flows under different feasible operating conditions [3]. Three-phase power flow will struggle to adequately assess the challenges presented by BEV and DER growth because scenarios requiring upgrades might fail to converge due to an infeasible network with unsatisfied AC network constraints. For example, simulation alone cannot identify optimal locations for needed infrastructure upgrades that will increase electric load, like fast charging stations, or areas of weakness due to insufficient reactive power compensation in the network. Tools for distribution grid power flow offer limited, if any, optimization capabilities [3]. New distribution planning tools and capabilities are needed that are

capable of running optimizations while satisfying three-phase AC unbalanced network constraints. These new tools will help system planners make optimal decisions on updating and installing new infrastructure when combined with operational, financial, and policy constraints [4].

While availability of such complete three-phase power flow tools are limited, three-phase optimization is an active and broad research area [5]. Several optimization approaches are targeted to three-phase optimal power flow (OPF), which typically minimizes economic dispatch subject to network constraints. These OPF methods have often been formulated using power balance network equations as seen in [6], which applies OPF to active distribution networks. The authors in [7] extend traditional power-balance constrained OPF to include slack variables that indicate constraint violations when there is no feasible solution. Other three-phase optimizations include technical objectives, like those that minimize losses [8], while still being subject to network equality constraints.

Formulations using power-balance equations [6] [7] [8] are highly nonlinear and therefore do not scale well in general. This behavior is shown in [9], which developed a four-wire OPF with both current-voltage (I-V) and power balance formulations and found that power-balance did not converge for 35% of testcases. Not only was I-V faster across the moderately sized testcases where power balance did converge, but the I-V formulation also returned more practical solutions. In the power balance formulation for 4-wire systems, some of the nodes were non-physically grounded, thereby resulting in erroneous voltage solutions [9]. Furthermore, many of these three-phase network-constrained optimizations will fail when there is no feasible power flow solution if slack variables or constraint violations are not considered.

A three-phase infeasibility analysis (TPIA) is another type of three-phase optimization formulated subject to current-based network constraints for use in distribution grid planning. TPIA localizes and identifies deficient areas, in addition to the *amount* of the deficiency, in situations where power flow fails [10]. At a high level, it is a non-convex optimization study that identifies scenarios where AC three-phase power flow constraints are infeasible by using a set of variable slack sources with a physical meaning to compensate for mismatch in the nodal equations. In TPIA, solutions with nonzero slack sources occur when power flow would otherwise fail.

Initially, the concept of quantifying infeasibility used power

\* denotes the corresponding author

balance network constraints for positive sequence systems to find a solvable boundary for otherwise insolvable power flow simulations [11]. We formulated an **infeasibility analysis** using slack current sources and KCL network constraints for transmission networks in [12] and three-phase networks in [10], where we additionally developed an L1-norm objective formulation that effectively localized the sources of infeasibility. Our work in [10] and [12] focused only on slack current models that can be directly added into the KCL network constraints. Neither work included any analysis on whether the algorithmic performance would change if slack current sources were replaced with either slack power or slack admittance sources, both of which can represent physical grid assets. In addition, operational constraints, like nodal voltages bounds, were not included in the prior formulation.

In this paper, we evaluate slack model choices by analyzing both problem complexity and real-world applications. We ensure the solutions from our TPIA formulations are feasible and actionable by using inequality constraints to incorporate bus voltage magnitude restrictions. We give insight into the mathematical complexity of each formulation in Section III and empirically verify computational complexity using convergence properties from infeasible networks in Section V. To evaluate the practicality of each slack source, we consider the relationship between physical assets that address real-world challenges, like capacitor banks, and the information provided from each TPIA formulation. We find that slack power or slack admittance best represent reactive power compensation because real power or conductance slack variables can be set to zero, which allows only reactive power slack injections.

## II. BACKGROUND

The background for this work is primarily the concept of infeasibility analysis and the circuit heuristics that are utilized for three-phase optimization.

### A. Infeasibility Analyses

Infeasibility analysis was first introduced for transmission networks in [11], and later in terms of an equivalent circuit for power grids in [12]. [12] introduced slack current sources at each node in the positive sequence circuit model of the power grid. It minimized the norm of the slack current sources to identify when positive sequence power flow was infeasible and returned the amount of missing current at each node in the system. [13] extended [12] to localize the sources of infeasibility by using an L1 regularization term in a least-squares objective. In [10], we introduced a scalable TPIA framework using three-phase current-based network constraints with two different objective functions; one using a least-squares objective and the other an L1-norm objective, which localized the solution to a subset of nodes.

However, the equivalent circuit approaches in [10] [12] [13] cannot directly relate slack source values with realizable physical assets on the grid. Furthermore, they do not enforce physical bounds on the grid voltages, thereby producing results with non-actionable infeasible solutions. Additionally,

minimizing current produces solutions where the net power injection might be impractical given the varying base voltages across the distribution grid (i.e., providing a 1 amp current injection at a 13.2 kV bus requires much more power than supplying 1 amp at a 240 V bus). In this paper, we address these limitations by: (a) formulating TPIA with alternative slack sources (slack admittance and power); (b) restructuring the objective function to minimize net complex power for all slack formulations; and (c) enforcing operational bounds using inequality constraints.

### B. Circuit Heuristics for Three-phase Optimization

We leverage and adapt some of techniques that have been used for circuit simulation to improve the performance of our three-phase power grid optimization. One such technique is homotopy, which we have adapted for power systems to attain convergence for difficult power flow and optimization problems. To mitigate the convergence challenges due to a lack of good initial guess, Tx-stepping (a power system specific homotopy method) begins by relaxing the network constraints by adding large admittances in parallel to all network branches and transformers, which effectively shorts most of the buses in the network. An analysis of the relaxed network is first solved and then the synthetic large admittance is gradually removed in small steps. The analysis is solved repeatedly using the prior solution as an initial guess for subsequent steps until the original complex problem is solved [14]. We will apply Tx-stepping to solve TPIA in this work. To further ensure robust convergence of TPIA when there are inequality constraints from operational limits, we further leverage a limiting technique for Newton-Raphson (NR) that is based on our understanding of individual device model characteristics. First developed for diodes, this heuristic dampens the update steps of primal and dual variables associated with inequality constraints so that their respective values never enter infeasible regions [15].

## III. METHODOLOGY

Next we describe three versions of the TPIA formulation using different slack sources: TPIA-I with slack current sources; TPIA-PQ with slack power sources; and TPIA-GB with slack admittance sources. Our prior work in [10] covered a version of TPIA-I, but for completeness, we reproduce it here. To ensure that various TPIA formulations provide meaningful solutions, we introduce operational limits in Section III-F.

In TPIA, if the network is feasible, the slack sources converge to zero. Otherwise, nonzero slack sources occur and can be used to identify and localize grid infeasibility for planning insight or corrections during operation. In this paper, we consider various slack formulations to compare their solution complexity and practical applicability in grid operation and planning. All three model formulations provide flexibility to impose upper and lower limits on the slack resources (e.g., constraining a susceptance  $B$  per phase  $\phi$  by its upper rating:  $B_s^\phi \leq \overline{B_s^\phi}$  [16]).

### A. Three-Phase Power Flow Constraints

We use nonlinear KCL network equations to represent the steady-state grid physics in the TPIA formulations. Due to the modular circuit-based approach, the TPIA framework can model any three-wire or four-wire distribution feeders with various transformer configurations and distribution assets like inverter based distributed generators, voltage regulators, triplex loads, capacitors, fuses, shunts, and switches. The models for these devices are detailed in [17].

We describe the KCL-based three-phase AC network constraints in (1) and (2), where  $f_r^\phi(x)$  and  $f_i^\phi(x)$ , are the respective rectangular real and imaginary nodal current equations.  $x$  is a vector of power flow variables that includes the real and imaginary voltages,  $V_R^\phi$  and  $V_I^\phi$ , per phase  $\phi$ .  $G$  and  $B$  are matrices of network conductances and susceptances.  $I_R^{NL}$  and  $I_I^{NL}$  are nonlinear currents from either PV or PQ buses, but for brevity, we represent them as though they are from PQ buses and omit the reactive power variable and voltage setpoint equation for PV buses. Given a solution  $x$  for a feasible network,  $f_r^\phi(x)$  and  $f_i^\phi(x)$  are equal to 0, but in infeasible networks, there will be a nonzero mismatch at some of the nodal equations.

$$f_r^\phi(x) = GV_R^\phi - BV_I^\phi + I_R^{NL}(V_R^\phi, V_I^\phi) = 0 \quad (1)$$

$$f_i^\phi(x) = BV_R^\phi + GV_I^\phi + I_I^{NL}(V_R^\phi, V_I^\phi) = 0 \quad (2)$$

The vectorized nonlinear current equations  $I_R^{NL}$  (3) and  $I_I^{NL}$  (4) are functions of power injections. We later define slack power sources with a modified version of (3) and (4).

$$I_R^{NL}(V_R^\phi, V_I^\phi) = (P^\phi \odot V_R^\phi + Q^\phi \odot V_I^\phi) \odot ((V_R^\phi)^2 + (V_I^\phi)^2) \quad (3)$$

$$I_I^{NL}(V_R^\phi, V_I^\phi) = (P^\phi \odot V_I^\phi - Q^\phi \odot V_R^\phi) \odot ((V_R^\phi)^2 + (V_I^\phi)^2) \quad (4)$$

### B. General TPIA Format

The general format for TPIA stays the same across the different slack variable formulations. The objective function in 5a represents the sum of squares of the complex power injection,  $g_m^\phi(s)$ , by the set of slack variables  $s$  for all  $n$  buses and all connected phases  $\phi$ . We select this objective function to address some of the challenges discussed in Section II-A. The variable  $\alpha$  represents a scaling parameter necessary to ensure robust convergence in the presence of inequality constraints. Each formulation is subject to the network constraints modified by  $h_r^\phi(s)$  and  $h_i^\phi(s)$ , which represent the real (5b) and imaginary (5c) current injections from each slack source.

$$\min \sum_{m=1}^n \sum_{\phi \in \{A, B, C\}} \alpha g_m^\phi(s) \quad (5a)$$

$$\text{s.t. } f_r^\phi(x) - h_r^\phi(s) = 0 \quad (5b)$$

$$f_i^\phi(x) - h_i^\phi(s) = 0 \quad (5c)$$

The functions for  $g_m^\phi(s)$ ,  $h_r^\phi(s)$ , and  $h_i^\phi(s)$  will change depending on the choice of slack source. This is to ensure that we compare equivalent quantities in the objective.

Although it can be shown that the subsequent three formulations for TPIA-I, TPIA-PQ, and TPIA-GB are mathematically equivalent, the reformulations can affect the nonlinearities in the objective function and the constraints, and with different initial conditions, the choice of formulation can result in a different solution trajectory.

### C. TPIA-I Formulation

In TPIA-I, we use real and imaginary slack current sources,  $i_{fR}^\phi$  and  $i_{fI}^\phi$ , to develop insight into how much current (or post-processed power) is needed at a given location. The objective function sums  $g_m^\phi(s)$ , which is the square of complex power at node  $m$  and phase  $\phi$  (6a). Complex power is calculated by the product of complex voltage and conjugate complex current. The current injections in (6b) and (6c) are simply defined by slack current sources themselves.

$$g_m^\phi(s) = \left( (i_{fR,m}^\phi)^2 + (i_{fI,m}^\phi)^2 \right) \left( (V_{R,m}^\phi)^2 + (V_{I,m}^\phi)^2 \right) \quad (6a)$$

$$h_r^\phi(x) = i_{fR}^\phi \quad (6b)$$

$$h_i^\phi(x) = i_{fI}^\phi \quad (6c)$$

Overall, the slack current sources add the least complexity to the network constraints by introducing only linear terms but greater nonlinear complexity to the objective because of the product of squared variables. It is important to note, however, that TPIA-I cannot restrict injections to only reactive power without introducing additional nonlinear constraints that set real power to zero.

### D. TPIA-PQ Formulation

TPIA-PQ can provide the same insight as TPIA-I but has expanded use-cases when considering real-world assets that provide only reactive power compensation like static synchronous compensators (STATCOMs). The objective function sums  $g_m^\phi(s)$ , which is the individual squares of the real and reactive slack power sources,  $P_s$  and  $Q_s$ , at bus  $m$  and phase  $\phi$  (7a). The KCL current injections from the slack power sources,  $I_R^s$  (7b) and  $I_I^s$  (7c), are equivalent to (3) and (4) except the original constants  $P$  and  $Q$  are now variables  $P_s$  and  $Q_s$ .

$$g_m^\phi(s) = (P_{s,m}^\phi)^2 + (Q_{s,m}^\phi)^2 \quad (7a)$$

$$h_r^\phi(x) = I_R^s(V_R^\phi, V_I^\phi, P_s^\phi, Q_s^\phi) \quad (7b)$$

$$h_i^\phi(x) = I_I^s(V_R^\phi, V_I^\phi, P_s^\phi, Q_s^\phi) \quad (7c)$$

Slack power sources introduce the most complexity to the KCL equations since they are rational functions of voltages with a sum of squares in the denominator. However, the objective function is only quadratic, which makes it the least complex of the three formulations. TPIA-PQ can model only reactive power injections by simply setting  $P_{s,m} = 0$  at each bus  $m$ . This formulation, which we call TPIA-Q, requires no additional constraints.

### E. TPIA-GB Formulation

Since system planners might want to explore installing capacitor banks for reactive power compensation, we develop an admittance-based TPIA formulation. In TPIA-GB, we use

slack conductance  $G_s$  and slack susceptance  $B_s$  variables to represent the slack admittance sources. The objective function sums  $g_m^\phi(s)$ , which is the product of admittance and squared voltages at bus  $m$  and phase  $\phi$  (8a). The current injections from the slack admittance sources are found by multiplying voltage and admittance in (8b) and (8c).

$$g_m^\phi(s) = ((G_{s,m}^\phi)^2 + (B_{s,m}^\phi)^2) \left( (V_{R,m}^\phi)^2 + (V_{I,m}^\phi)^2 \right)^2 \quad (8a)$$

$$h_r^\phi(x) = -G_s^\phi \odot V_R^\phi + B_s^\phi \odot V_I^\phi \quad (8b)$$

$$h_i^\phi(x) = -G_s^\phi \odot V_I^\phi - B_s^\phi \odot V_R^\phi \quad (8c)$$

The terms added to the network constraints by slack admittance sources are bilinear, which is less complex than terms added by TPIA-PQ, but more complex than TPIA-I. However, (8c) is the most nonlinear objective of the three formulations. While TPIA-GB includes both  $G_s$  and  $B_s$ , we recognize that a formulation including only  $B_s$  is more realistic since it represents capacitive behavior. To allow only reactive power compensation, we develop TPIA-B, which requires no additional constraints and sets  $G_{s,m} = 0$  on all buses.

#### F. Operational Limits

Formulations in Sections III-C through III-E may help identify infeasible networks, but their output may not be usable by grid planners. In some particularly stressed networks, the bus voltage magnitudes in a TPIA solution may lie outside of the acceptable range, rendering any information from TPIA frameworks non-actionable. Therefore, to ensure that bus voltage magnitudes are within specific ranges, we include inequality constraints on the bus voltage magnitudes for all  $n$  buses and phases  $\phi$ . In (9),  $\underline{V}_i^\phi$  and  $\overline{V}_i^\phi$  are the constant-valued lower and upper voltage magnitude bounds:

$$(\overline{V}_i^\phi)^2 \leq (V_{R,i}^\phi)^2 + (V_{I,i}^\phi)^2 \leq (\underline{V}_i^\phi)^2, \quad \forall i \in n \quad (9)$$

(9) introduces additional nonlinearities to TPIA, so heuristics from Section II-B are necessary for robust convergence.

#### G. Optimization Solution Quality

For each of the above formulations, we solve the optimization problem using the primal-dual interior point (PDIP) approach [18] aided by the circuit-simulation heuristics from Section II-B. We seek a local minimizer by solving for a set of primal and dual variables that satisfy the perturbed first-order KKT conditions of the Lagrangian. The underlying problem is non-convex due to nonlinear network constraints, so no standard approach exists to obtain the global optima. However, our prior works in [17] and [19] have proposed heuristics that can be used to improve convergence to practical and meaningful solutions and to avoid saddle points.

### IV. EXPERIMENTAL SET-UP

To evaluate the computational efficiency of the TPIA formulations, we incorporated the new models and techniques into our three-phase power grid implementation in [20]. Specifically, we implemented TPIA-PQ, TPIA-GB, and TPIA-I formulations with a common objective and enforced voltage

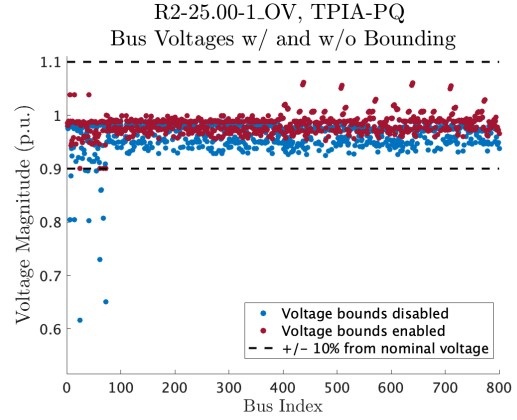


Fig. 1. The impact of TPIA-PQ injections on satisfying bus voltage magnitude limits for R2-25.00-1\_OV.

bounds. We tested our approaches on the PNNL taxonomy feeders, where modifications are made to some of them to increase the load factor to stress the networks and induce infeasibility [21]. The testcases are available at [22] and described in [10]. They represent a small urban center on the U.S. West Coast with 76 nodes (R1-12.47-3\_OV); an urban area in the U.S. Northeast with 800 nodes (R2-25.00-1\_OV); and an urban area with rural spur in the U.S. Southeast with 1599 nodes (R4-12.47-1), which is the original version of the testcase and exhibits solutions with voltages outside of operational ranges.

For consistency, we include slack variables at all nodes in the system. However, in TPIA, slack variables can be included at only a subset of system nodes based on the planner's or operator's knowledge. To demonstrate our operational bounds, we used 0.9 per unit (p.u.) of the nominal bus voltage for  $\underline{V}_i^\phi$  and 1.1 p.u for  $\overline{V}_i^\phi$  for all results except in the reactive power use case where voltage bounds are more strictly defined. Diode limiting is used for all voltage-bounded formulations. Tx-stepping is only used when explicitly mentioned.

### V. RESULTS & DISCUSSION

Here we show the results and discuss performance and practical considerations for the TPIA formulations.

#### A. Impact of Voltage Bounds

Fig. 1 demonstrates the impact of voltage bounding on the solution for R2-25.00-1\_OV. In this case, 13 buses have at least one phase with a voltage magnitude below 10% of its nominal value, as shown by the blue dots. When voltage limits are included, all bus voltage magnitudes (red dots) are kept within  $\pm 10\%$  by introducing infeasibility injections of 18% and 35% of the total P and Q consumed by the feeder, respectively.

Since omitting voltage limits may lead to non-actionable solutions, the following results include voltage limits for all cases. Fig. 2 shows the number of iterations it took for TPIA-I, TPIA-PQ, and TPIA-GB to converge for the three infeasible networks. TPIA-PQ took the fewest iterations.

The formulations also yielded varying performances regarding the amount of power required to make the network feasible. Table I reports the sum of absolute values of the

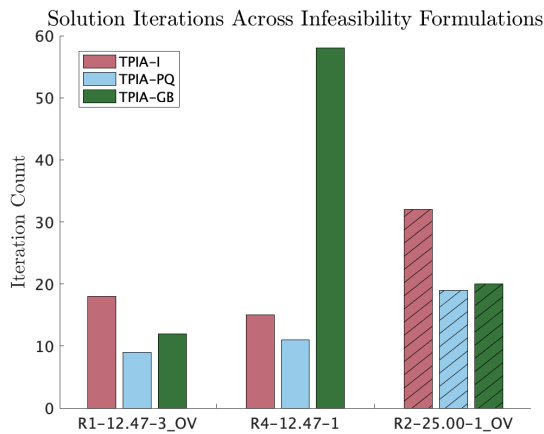


Fig. 2. NR iterations in our PDIP solver [20] for convergence of each TPIA formulation and testcase. Hatched filling implies that Tx-stepping was needed.

complex power from infeasibility sources dispatched across all cases and formulations. While the optimization sought to minimize the sum of squares of complex power injections, we report the simple sum because those values are more intuitive for grid planning. For these cases, TPIA-PQ and TPIA-GB mostly generate solutions with less slack power dispatched than TPIA-I.

TABLE I  
TOTAL COMPLEX POWER INJECTIONS

Case	TPIA-I	TPIA-PQ	TPIA-GB
	$\Sigma S_f$ (kVA)	$\Sigma S_f$ (kVA)	$\Sigma S_f$ (kVA)
R1-12.47-3_OV	6.78e3+j4.65e3	2.03e2+j2.39e2	2.03e2+j4.34e2
R2-25.00-1_OV	1.52e4+j1.03e4	5.81e3+j1.07e4	5.69e3+j1.26e4
R4-12.47-1	8.90e2+j8.40e2	1.37e3+j1.81e2	1.16e2+j1.93e2

### B. Reactive Power Compensation Use-Case

TPIA can help grid planners with optimal reactive power compensation. To demonstrate its utility, we used the testcase R4-12.47-1, which, without reactive power compensation, has 12 system buses (out of 1599 nodes) outside of 0.95 and 1.05 p.u. voltage range, a range commonly enforced by real-world utilities. To enforce the voltages with reactive power compensation, we ran TPIA-B and found that the network needed 5 MVAR of reactive power to achieve acceptable voltages. We then modified the testcase to include 40 capacitors based on values from the TPIA-B solution and placed them at their respective locations. We subsequently ran the modified testcase in TPIA-B without voltage bounds, where it converged in 4 iterations and had all bus voltages between 0.95 and 1.05 p.u. without needing any infeasibility injections (which is indicative of a power flow solution).

## VI. CONCLUSION

Three-phase analysis tools used for distribution grid planning must evolve to account for the growing complexity at the grid edge. We developed a three-phase infeasibility analysis with current, power, and admittance slack models that can provide insight on where infeasibilities occur and the extent of the infeasibility. To produce realistic results, we construct voltage bounds for each formulation. We find that the formulations

with slack reactive power or admittance can be modified to represent specific reactive power assets like STATCOMs and capacitors, respectively. Across the testcases that we studied, the voltage-bounded slack power formulation converged the fastest and both voltage-bounded slack power and admittance formulations generally returned smaller net complex power injections than the voltage-bounded slack current formulation.

## REFERENCES

- [1] International Energy Agency, "Global EV Outlook 2021", April 2021. Available: <https://www.iea.org/reports/global-ev-outlook-2021>.
- [2] National Academy of Sciences, Engineering, and Medicine. *The Future of Electric Power in the United States*. Washington, D.C: the National Academies Press, 2021.
- [3] J. S. Homer, et. al. "Electric Distribution System Planning with DERs-High-level Assessment of Tools and Methods", Pacific Northwest National Lab, Richland, WA, March 2020.
- [4] "Reimagining the Grid". Southern California Edison, Rosemead, CA, USA. Dec. 2020 [Online]. Available: <https://www.edison.com/home/our-perspective/reimagining-the-grid.html>
- [5] A. Keane et al., "State-of-the-Art Techniques and Challenges Ahead for Distributed Generation Planning and Optimization," *IEEE Trans. on Power Sys.*, vol. 28, no. 2, May 2013.
- [6] S. Gill, I. Koccar, and G. Ault. "Dynamic Optimal Power flow for Active Distribution Networks," *IEEE Trans. on Power Sys.*, vol. 29, no. 1, Jan. 2014.
- [7] A. S. Zamzam, N. D. Sidiropoulos, and E. Dall'Anese, "Beyond Relaxation and Newton-Raphson: Solving AC-OPF for Multi-Phase Systems with Renewables," *IEEE Trans. on Smart Grid*, vol. 9, no. 5, Sept. 2016.
- [8] L. Ochoa and G. Harrison, "Minimizing Energy Losses: Optimal Accommodation and Smart Operation of Renewable Distributed Generation," *IEEE Trans. on Power Sys.*, vol. 26, no. 1, Feb. 2011.
- [9] S. Claeys, F. Geth, and G. Deconinck, "Optimal Power Flow in Four-Wire Distribution Networks: Formulation and Benchmarking," *Electric Power Sys. Res.*, vol. 213, Dec. 2022.
- [10] E. Foster, A. Pandey, and L. Pileggi, "Three-Phase Infeasibility Analysis for Distribution Grid Studies," *Electric Power Sys. Res.*, vol. 212, Nov. 2022.
- [11] T. J. Overbye, "A power flow measure for unsolvable cases," *IEEE Trans. on Power Systems*, vol. 9, no. 3, Aug. 1994.
- [12] M. Jereminov, D. M. Bromberg, A. Pandey, M. R. Wagner and L. Pileggi, "Evaluating Feasibility Within Power Flow," *IEEE Trans. on Smart Grid*, vol. 11, no. 4, July 2020.
- [13] S. Li, A. Pandey, A. Agarwal, M. Jereminov and L. Pileggi, "A LASSO-Inspired Approach for Localizing Power System Infeasibility," presented at 2020 *IEEE PES General Meeting*, Montreal, QC, Canada, Aug. 2-6, 2020.
- [14] A. Pandey, M. Jereminov, M. R. Wagner, G. Hug and L. Pileggi, "Robust Convergence of Power Flow Using TX Stepping Method with Equivalent Circuit Formulation," presented at the Power Sys. Comp. Conf. (PSCC), Dublin, Ireland, June 11-15, 2018.
- [15] M. Jereminov, A. Pandey, and L. Pileggi, "Equivalent Circuit Formulation for Solving AC Optimal Power Flow," *IEEE Trans. on Power Sys.*, vol. 34, no. 3, May 2019.
- [16] *IEEE Standard for Shunt Power Capacitors*, IEEE Std 18-2012 (Revision of IEEE Std 18-2002), Feb. 15, 2013.
- [17] A. Pandey, et al., "Robust Power Flow and Three-Phase Power Flow Analyses," in *IEEE Trans. on Power Sys.*, vol. 34, no. 1, Jan. 2019.
- [18] S. Boyd, S. P. Boyd, and L. Vandenberg, *Convex Optimization*, Cambridge University Press, 2004.
- [19] T. McNamara, A. Pandey, A. Agarwal, and L. Pileggi, "Two-stage homotopy method to incorporate discrete control variables into AC-OPF," *Electric Power Sys. Res.*, vol. 212, Nov. 2022.
- [20] A. Pandey, N. Turner-Bandele, E. Foster, and T. McNamara, *SUGAR-D: A Distribution Systems Analysis and Optimization Tool v2.02*, CMU ECE Pileggi Lab Group, Pittsburgh, PA, 2022.
- [21] K.P. Schneider, et al., "Modern Grid Initiative Distribution Taxonomy Final Report," Pacific Northwest National Lab, Richland, WA, Nov. 2008.
- [22] E. Foster, TPIA Experiment Testcases, 2022, Github Repository. <https://github.com/emfoster/TPIA-Experiment-Testcases>